Cell Stress and Chaperones (2018) 23:813–826
https://doi.org/10.1007/s12192-018-0890-5

ORIGINAL PAPER

Small heat shock protein speciation: novel non-canonical 44 kDa HspB5-related protein species in rat and human tissues

Rainer Benndorf[1] · Robert R. Gilmont[2] · Sahoko Hirano[1] · Richard F. Ransom[3] · Peter R. Jungblut[4] · Martin Bommer[5] · James E. Goldman[6] · Michael J. Welsh[1]

Received: 23 January 2018 / Revised: 21 February 2018 / Accepted: 23 February 2018 / Published online: 14 March 2018

Abstract

When analyzing small stress proteins of rat and human tissues by electrophoretic methods followed by western blotting, and using the anti-HspB1/anti-HspB5 antibody clone 8A7, we unexpectedly found a protein with a molecular mass of ~44 kDa. On two-dimensional gels, this protein resolved into four distinct species. Electrophoretic and immunological evidence suggests that this 44 kDa protein is a derivative of HspB5, most likely a covalently linked HspB5 dimer. This HspB5-like 44 kDa protein (HspB5L-P44) is particularly abundant in rat heart, brain, and renal cortex and glomeruli. HspB5L-P44 was also found in human brains, including those from patients with Alexander disease, a condition distinguished by cerebral accumulation of HspB5. Gray matter of such a patient contained an elevated amount of HspB5L-P44. A spatial model of structurally ordered dimeric HspB5 α-crystallin domains reveals the exposed and adjacent position of the two peptide segments homologous to the HspB1-derived 8A7 antigen determinant peptide (epitope). This explains the observed extraordinary high avidity of the 8A7 antibody towards HspB5L-P44, as opposed to commonly used HspB5-specific antibodies which recognize other epitopes. This scenario also explains the remarkable fact that no previous study reported the existence of HspB5L-P44 species. Exposure of rat endothelial cells to UV light, an oxidative stress condition, temporarily increased HspB5L-P44, suggesting physiological regulation of the dimerization. The existence of HspB5L-P44 supports the protein speciation discourse and fits to the concept of the protein code, according to which the expression of a given gene is reflected only by the complete set of the derived protein species.

Keywords Protein modification · Covalently bonded HspB5 dimers · HspB1-/HspB5-specific antibody clone 8A7 · Protein speciation · Mammals

Rainer Benndorf and Robert R. Gilmont contributed equally to this study.

Rainer Benndorf and Michael J. Welsh are retired.

Robert R. Gilmont is deceased. The remaining authors wish to dedicate this study to him.

✉ Rainer Benndorf
rbenndo@gmx.net

[1] Department of Cell and Developmental Biology, University of Michigan Medical School, Ann Arbor, MI, USA

[2] Department of Plastic and Reconstructive Surgery, University of Michigan Medical School, Ann Arbor, MI, USA

[3] Department of Pharmacology, University of Michigan Medical School, Ann Arbor, MI, USA

[4] Core Facility Protein Analysis, Max-Planck-Institute for Infection Biology, Berlin, Germany

[5] Max-Delbrück-Centrum für Molekulare Medizin, Berlin, Germany

[6] Department of Pathology and Cell Biology, Columbia University, New York, NY, USA

Introduction

Mammalian genomes encode ten small heat shock proteins (sHSP), now systematically named HspB1 through HspB10 (Kampinga et al. 2009). sHSPs are defined by a highly conserved ~85 amino acid residue sequence element called α-crystallin domain which is typically encompassed by a less conserved N-terminal domain and a poorly conserved and highly flexible region of C-terminal extensions (Fontaine et al. 2003; Benndorf et al. 2014). In humans and rats, HspB5 (αB-crystallin) is encoded by the *CRYAB* and *Cryab* gene, respectively. HspB5, together with the related HspB4, was discovered in the lens of the eye more than a century ago and belongs historically to the first proteins to be known (Mörner 1893). Today, we know that HspB5 occurs in many organs and tissues at "baseline" conditions (Lowe et al. 1992a; Klemenz et al. 1993), in some cases in extraordinary high amounts (Kato et al. 1991), and its synthesis can be further induced by a number of stress conditions, including oxidative stress and various neuropathologies (Klemenz et al. 1991; Iwaki et al. 1992, 1993; Renkawek et al. 1992; Lowe et al. 1992a, 1992b). At the molecular level, the best studied functions of HspB5 include its chaperone-like activity and its role in the organization of the cytoskeleton, notably the intermediate filaments (Mymrikov et al. 2011; Elliott et al. 2013; Haslbeck et al. 2016). The *CRYAB* gene is affected in humans by a number of mutations that result in various myopathies and in the formation of cataracts in the lens of the eye (Benndorf 2010; Datskevich et al. 2012; Benndorf et al. 2014).

Like most if not all sHSPs, HspB5 forms dimers and oligomeric complexes of variable size, be they homologous or heterologous dimers or oligomeric complexes with other sHSPs (Mymrikov et al. 2011). This quaternary structure of sHSPs has been extensively studied (Behlke et al. 1995; Bagnéris et al. 2009; Jehle et al. 2010; Aquilina et al. 2013; Delbecq et al. 2015), and it is thought that dimers are the basic building block of such oligomeric sHSPs. For HspB5, all naturally occurring dimers and oligomeric complexes reported to date are formed by association without involvement of a covalent bond as they can be dissociated by breaking the hydrophobic and hydrogen bonds with detergents and urea, respectively, such as applied during electrophoretic procedures. Covalently bonded dimers have been found only after chemical oxidation of mixed populations of HspB5 and HspB4 (Balasubramanian and Kanwar 2002; Shum et al. 2005). Apart from those studies, we could not find any other reports on covalently bonded HspB5 dimers.

In the past decade, it became clear that commonly determined gene expression often falls short in terms of understanding the functions of a given protein in live cells (Jungblut et al. 2016). Instead, the entirety of the derived forms of a protein (protein species[1]) seems critical for its function. These protein species are generated by various modifications, splicing, and/or truncations, eventually resulting in a tremendous diversification of a given protein. This development has opened a whole new world "below" the level of the proteins, and the resulting protein speciation discourse has led to the concept of the protein code. Examples include the diversity of the histones (Jungblut et al. 2016), but also of HspB1 of which at least 59 and 15 species have been found in the human heart and in murine Ehrlich ascites tumor cells, respectively (Benndorf et al. 1992; Scheler et al. 1997; Benndorf and Jungblut 2015). Conceptually, we distinguish between commonly observed (canonical) and rarely or newly observed (non-canonical) protein species.

Here we report a novel 44 kDa protein which is, according to electrophoretic and immunological evidence, related to HspB5 and most likely a covalently linked HspB5 dimer. This protein occurs in a number of rat tissues, and also in healthy and diseased human brains, with the latter known to accumulate abnormal amounts of HspB5. The discovery of this protein was by chance when we studied the sHSP expression in rat tissues using the monoclonal anti-HspB1-/HspB5-specific antibody clone 8A7 which was raised against a short peptide derived from the α-crystallin domain of human HspB1. This antibody exhibits an extraordinary high avidity towards this HspB5-related 44 kDa protein, as compared to the canonical HspB5 species, and as compared to an HspB5-specific antibody which was raised against a peptide derived from the C-terminal extension of human HspB5. Analyzing the positions of the epitopes for both antibodies in spatial models of HspB5, we provide a rationale for the observed high avidity of the 8A7 antibody towards this novel HspB5-derived protein, and also for the remarkable fact that this protein was not noticed in the numerous earlier studies on HspB5. Our findings on this novel HspB5 species further support the protein speciation discourse and fit with the concept of the protein code.

[1] According to the IUPAC-IUBMB Joint Commission on Biochemical Nomenclature rules (Nomenclature of multiple forms of enzymes. In: Biochemical nomenclature and related documents, 2nd edition. Edited by: Liébecq C. Colchester; Portland press; 1992), we refer to differentially modified protein forms as "protein species," as we have justified before (Benndorf and Jungblut 2015). The term isoform should be restricted to genetic variants. We refer to newly observed or rare protein species as "non-canonical protein species" which are typically found in non-canonical spots on two-dimensional gels, as opposed to the "canonical protein species" which designates the traditionally observed protein species that are found in the canonical spots on two-dimensional gels. It should also be noted that a single protein spot on two-dimensional gels may contain more than one protein species (Jungblut et al. 2008).

Methods

Human patients

We examined frozen tissues of the central nervous system (CNS), including isocortex and subcortical white matter, taken at autopsy from three patients with genetically caused Alexander disease (AXD): a 7-year-old male and an 8-year-old female with an R416W *GFAP* mutation each, and a 9-year-old female with an R239C *GFAP* mutation. For control purposes, we examined CNS tissues from a 2-year-old female with no neuropathology and from an 8-year-old male with X-linked adrenoleukodystrophy (ALD). All AXD patients showed the typical loss of myelin in white matter with many astrocytes with Rosenthal fibers, and many subpial astrocytes with Rosenthal fibers. The patient with ALD also showed loss of myelin and astrocytic gliosis in white matter, but no Rosenthal fibers.

Tissue sampling and extraction procedures

Tissues were harvested from two male Wistar rats of ~200 g weight, washed in saline, and snap frozen in liquid nitrogen. Renal cortex, medulla, and glomeruli were prepared as described previously (Smoyer et al. 2000; Guess et al. 2010). Approximately 40,000 renal glomeruli were isolated from two kidneys under semi-sterile conditions, and the preparation was assessed by microscopic inspection and contained ~95% glomeruli. Protein extraction was essentially as described earlier (Guess et al. 2013). In brief, tissues were homogenized at 4 °C in tissue protein extraction reagent T-PER (Pierce, Rockford, Illinois) in the presence of protease inhibitors (Sigma-Aldrich, St. Louis, Missouri) at 20 ml per gram tissue, using a Dounce homogenizer. Lysates were centrifuged at 14,000*g* for 5 min, and aliquots of the supernatant were stored at − 80 °C. For two-dimensional polyacrylamide gel electrophoresis (2D-PAGE), homogenates were adjusted to 6 M urea, 2% ampholytes 3–10, 2% Triton X-100, and 10 mM dithiothreitol (final concentrations), containing 3.3 mg/ml total protein. For SDS-polyacrylamide gel electrophoresis (SDS-PAGE), homogenates were mixed with 5 × SDS sample buffer, yielding a final concentration of 1.0 mg/ml total protein in 62.5 mM Tris-HCl (pH 6.8), 2% SDS, 10% glycerol, 5% β-mercaptoethanol, and 0.05% bromophenol blue. Before loading, the SDS samples were heated for 4 min in a water bath at 100 °C. Saline-washed and snap frozen human brain samples were processed for SDS-PAGE like the rat tissues.

Endothelial cell culture

4×10^5 rat pulmonary arterial endothelial cells (passages 10 to 16) were plated into each well of 6-well plates and grown in a 1:1 mix of Ham's F12:Dulbecco's Modified Eagle Medium (GibcoBRL, Grand Island, New York) supplemented with 5% fetal calf serum, 50 μg/ml penicillin, and 50 μg/ml streptomycin, for 96 h in a humidified atmosphere of 5% CO_2 at 37 °C prior to the assay (Gilmont et al. 1996; Hirano et al. 2004). For ultraviolet (UV) light exposures, the plates were placed without lid for 30 min in a biosafety cabinet under a UV lamp at an energy density of ~240 μW/cm^2 (manufacturer's specification). Thereafter, the cells were returned to the incubator and allowed to recover for up to 24 h. At the indicated time points, the culture medium was aspirated and cells were washed twice with PBS, detached from the support with a cell scraper, and collected by centrifugation. Cells were lysed by adding 200 μl tissue protein extraction reagent and processed for SDS-PAGE as described above.

Electrophoretic methods

2D-PAGE was conducted using the Multiphor II Electrophoresis System from Amersham Biosciences (GE Healthcare, Uppsala, Sweden) with Immobiline dry strips (3–10) for separation of the proteins by their isoelectric points (pI) in the first dimension. Subsequently, these strips were mounted onto the slab gels containing 0.1% SDS for the separation of the proteins according to their relative molecular masses (M*r*). For SDS-PAGE, 30 μg total protein (unless specified otherwise) was loaded onto 10% polyacrylamide gels according to standard procedures. After the run, the proteins were electrotransferred onto polyvinylidene difluoride (PVDF) membranes for immunolabeling (western blotting). The apparent molecular masses and isoelectric points were estimated by using reference proteins. Purified HspB5 was purchased from StressGen Biotechnologies, Victoria, British Columbia. The entire procedures were described in detail elsewhere (Benndorf et al. 2000).

The relative amounts of 8A7-reactive proteins in the various rat tissues were semi-quantitatively estimated by densitometry of the corresponding protein bands as obtained by western blotting. Developed X-ray films were scanned into files using a GS 200 Imaging Densitometer (Bio-Rad, Hercules, California) controlled by the accompanying software and using standard settings. The densitometric analysis was performed using the ImageJ program (version 1.46r) which is available at http://rsb.

info.nih.gov/ij/. The signal intensity obtained for the putative HspB5 dimer (HspB5-L-P44) was related to the signal intensity obtained for monomeric HspB5 in the same sample, and expressed as a ratio. Comparison of these numeric values from different tissues is informative with respect to the relative ratios; however, these values do not allow any conclusion about the absolute amounts of the corresponding proteins in the samples.

Antibodies

The mouse monoclonal anti-HspB1/anti-HspB5 antibody clone 8A7 was obtained from StressMarq Biosciences Inc., Victoria, British Columbia (catalog no. SMC-114). This antibody was raised against the epitope peptide KHEERQDEHGYISRC derived from human HspB1 (positions 123–137) (Bitar et al. 1991; Jia et al. 2001), herein referred to as the 8A7 antigen determinant peptide (8A7-ADP). Because this selected 8A7-ADP sequence is evolutionarily highly conserved, the 8A7 antibody cross-reacts also with the homologous 8A7-ADPs (ho-ADP) of HspB1 and HspB5 of a number of other mammalian species (including rats), albeit partially with reduced intensity.

The used HspB5-specific rabbit polyclonal anti-HspB5 antibody was kindly provided by Dr. J. Horwitz, The Jules Stein Eye Institute, University of California Los Angeles, Los Angeles, California. This antibody was raised against the epitope peptide REEKPAVTAAPKK which represents the uttermost C-terminal end of human HspB5, herein referred to as anti-HspB5 antigen determinant peptide (aB5-ADP) (Bhat et al. 1991). Based on the strong sequence similarity among mammalian HspB5 (Benndorf et al. 2014), this antibody reacts also with HspB5 of other species, including rats.

Secondary antibody solutions contained either peroxidase-conjugated goat anti-rabbit (dilution 1:10,000) or goat anti-mouse (dilution 1:10,000) antibodies, both from Jackson ImmunoResearch Laboratories (West Grove, Pennsylvania). Antibody binding was visualized with the ECL chemiluminescence system from GE Healthcare Bio-Sciences (Piscataway, New Jersey) and detected by exposure to X-ray film.

2D-PAGE database search

Among the numerous developed 2D-PAGE databases, only a few are still accessible today, including the World 2D-PAGE database (http://world-2dpage.expasy.org/swiss-2dpage), the 2D-PAGE database at MPIIB (http://www.mpiib-berlin.mpg.de/2D-PAGE/), the Reproduction 2D-PAGE database (http://reprod.njmu.edu.cn/), and the UCD 2D-PAGE database (http://proteomics-portal.ucd.ie/). These databases were queried using the keywords alphaB crystallin and CryAB, as well as the accession numbers P23927 and P02511 for mouse and human HspB5, respectively.

GenBank accessions

Human HspB5, NP_001876 (P02511); rat HspB5, NP_037067 (P23928); human HspB1, NP_001531 (P04792); rat HspB1, NP_114176 (P42930); mouse HspB5, NP_001276714 (P23927)

Results

Immunological and electrophoretic evidence for the existence of novel 44 kDa protein species related to HspB5 in rat tissues

Using 2D-PAGE followed by western blotting, we analyzed rat tissues for the occurrence of HspB1 and HspB5. For that purpose, we applied the monoclonal anti-HspB1/anti-HspB5 antibody clone 8A7 which was raised against the human HspB1-derived 8A7-ADP and which cross-reacts also with the ho-ADP sequences in rat HspB1 and rat HspB5 (cf. Methods section). As expected, in rat hearts, the 8A7 antibody detected the three canonical HspB1 spots at a M*r* of ~25 kDa (spot 1: pI~6.1, spot 2: pI~5.8, spot 3: pI~5.6), corresponding to non-phosphorylated, singly phosphorylated, and doubly phosphorylated HspB1 species, respectively. At a M*r* of ~22 kDa, the 8A7 antibody detected a single HspB5 spot (pI~6.8), corresponding to the canonical non-modified monomeric HspB5 species (Fig. 1). Similarly, in rat brains, this antibody labeled HspB1 which appeared only in spot 3, and non-modified monomeric HspB5.

Surprisingly, in both tissues, the 8A7 antibody strongly labeled additional protein species in the M*r* range of ~44 kDa, appearing in four spots (spot 1: pI~6.8, spot 2: pI~6.6, spot 3: pI~6.5, spot 4: pI~5.0) in the heart, and mainly in one spot (spot 3: pI~6.5) in the brain, with only faint labeling of spots 1 and 2 (Fig. 1). Additionally, in the brain, this antibody labeled a smear that "connects" the monomeric HspB5 spot with spot 1 of the 44 kDa protein, including a few discrete "intermediate protein species" (indicated by the bracket in Fig. 1).

For comparison, the same samples were analyzed by 2D-PAGE/western blotting using an antibody that is highly specific for HspB5 (cf. Methods section). As expected, this antibody labeled non-modified monomeric HspB5 at a M*r* of ~22 kDa (pI~6.8) in both tissues, but none of the HspB1 species (Fig. 1). However, a closer inspection revealed that

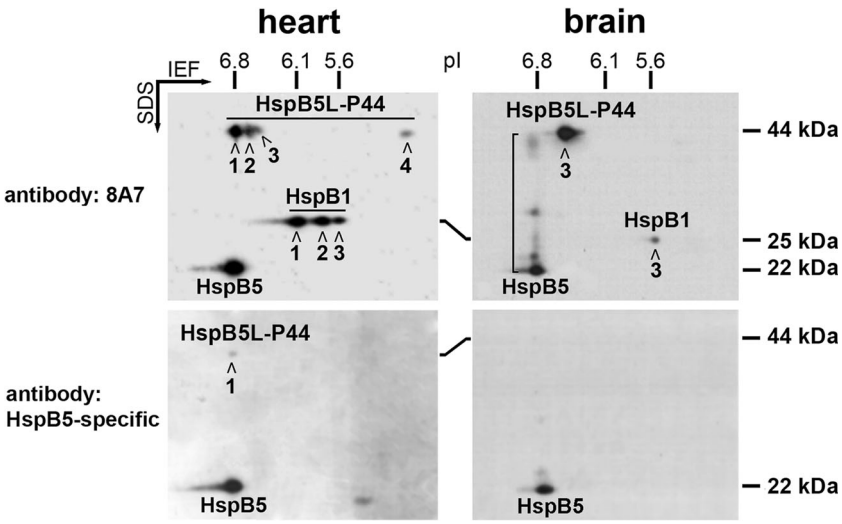

Fig. 1 Immunologic and 2D-PAGE evidence for an HspB5-related 44 kDa protein (HspB5L-P44) in rat heart and brain. The western blots were stained either with the 8A7 antibody (recognizes HspB5 and HspB1) or with the HspB5-specific antibody, as indicated. The positions of pI and M*r* standard proteins are marked. The "connecting smear" between the spots of monomeric HspB5 and of HspB5L-P44 in the brain sample, labeled by the 8A7 antibody, is indicated by the bracket

in rat hearts, this antibody labeled also the most abundant species of the 44 kDa protein in spot 1, albeit only slightly.

Together these findings suggest that the 44 kDa protein is related to HspB5, and most likely it is an HspB5 dimer. The arguments are the following: (i) The strong labeling by the 8A7 antibody implies that it contains the 8A7-ADP, or a closely related (homologous) sequence which must originate from an sHSP; (ii) The 44 kDa protein is also recognized, although weakly, by the highly specific anti-HspB5 antibody; (iii) The most abundant protein species in the heart in spot 1 has the same pI of ~6.8 as the non-modified monomeric HspB5; (iv) The 44 kDa protein species have approximately twice the M*r* compared to monomeric HspB5; and (v) The "connecting smear" seen in the brain sample. In the past, we have repeatedly observed such connecting smears on 2D-PAGE gels and blots between related protein species. An informative example is the smear that connects the HspB1 species contained in several spots on a two-dimensional gel (Benndorf and Jungblut 2015). Accordingly, the connecting smear shown in Fig. 1 suggests that the 44 kDa protein indeed is related to HspB5.

Since we could not find any earlier study reporting this protein in mammalian tissues, we termed it "HspB5-like 44 kDa protein" (HspB5L-P44), existing in at least four species which differ in their isoelectric points.

HspB5 is known to assemble into dimers and oligomeric complexes (cf. Introduction), and the presence of HspB5 dimers can be expected in physiological conditions in tissues. However, these dimers should completely dissociate into monomers in the presence of 6 M urea, 2% Triton-X100, 10 mM dithiothreitol, and 0.1% SDS during the sampling and electrophoretic procedures of the 2D-PAGE, resulting solely in the appearance of monomeric HspB5 on western blots of two-dimensional gels. The fact that HspB5L-P44 endured these procedures strongly suggests that this protein is formed by a covalent bond between the two HspB5 monomers, and not just by association, and thus represents a novel HspB5-like protein.

Figure 1 also implies that the 8A7 antibody is distinguished by its high affinity towards HspB5L-P44, as opposed to the HspB5-specific antibody which hardly recognized just the most abundant HspB5L-P44 species. Thus, the 8A7 antibody is a suitable tool for analyzing mammalian tissues for the presence of HspB5L-P44.

Subsequently, a larger number of rat tissues were analyzed by SDS-PAGE followed by western blotting for the presence of both HspB5L-P44 and HspB5 species, using the 8A7 antibody (Fig. 2). Confirming earlier results collected in rodents and humans (Dubin et al. 1989; Iwaki et al. 1992; Renkawek et al. 1992; Klemenz et al. 1993; Lutsch et al. 1997; Smoyer et al. 2000; van de Bovenkamp et al. 2006), strong to moderate signals for HspB5 were obtained in the lens of the eye, heart, skin, and spleen and in the renal compartments including cortex, glomeruli, and especially the medulla, whereas the lung, brain, and liver contained minor yet detectable amounts of HspB5.

The 8A7 antibody produced strong or moderate signals for HspB5L-P44 in the heart, lung, brain, renal cortex, and renal glomeruli, and faint signals in the eye lens, testis, liver, and skin, and also in commercially available HspB5 (Fig. 2). Interestingly, renal medulla which contains extraordinary high amounts of HspB5 (Smoyer et al. 2000) contains hardly any HspB5L-P44, which distinguishes this from the other renal compartments, the cortex and glomeruli. Apparently, HspB5L-P44 occurs in a number of rat tissues, albeit in different amounts.

The processing of these samples for the SDS-PAGE included a boiling step at 100 °C for 4 min in the presence of 2.0% SDS and 5% β-mercaptoethanol. The fact that the HspB5L-P44 endured also this harsh denaturing condition provides further and strong evidence that this HspB5 dimer is formed by a covalent bond.

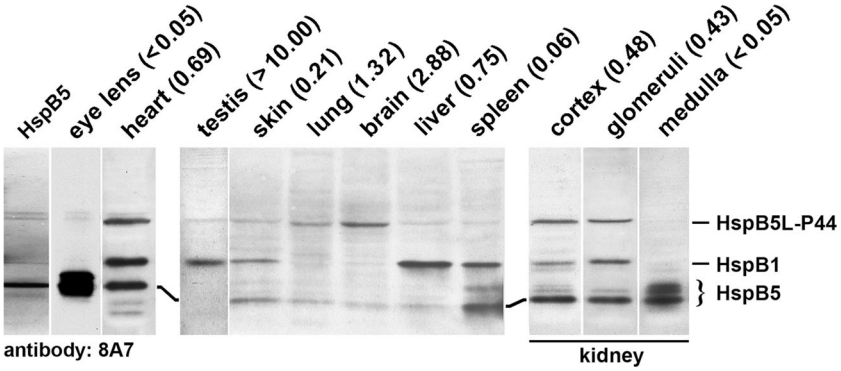

Fig. 2 Occurrence of HspB5L-P44 in various rat tissues. Purified HspB5 or proteins extracted from rat tissues were separated by SDS-PAGE, followed by western blotting using the 8A7 antibody. The total protein amounts loaded onto the lanes were 0.5 μg purified HspB5, 10 μg eye lens protein, and 30 μg protein from the other tissues. Distinct HspB5L-P44 signals were obtained in the heart, lung, brain, renal cortex, and renal glomeruli, and weak or negligible signals in the other tissues. The numeric values of the ratios of the signal strengths for both proteins (HspB5L-P44: HspB5) are given in parenthesis for each tissue

Although the affinities of the 8A7 antibody for both HspB5L-P44 and HspB5 are not known and can be assumed to differ greatly, Fig. 2 permits the conclusion that the relative amounts of HspB5L-P44 and HspB5 in the various tissues do not correlate. In the testis and brain, the HspB5L-P44 signals prevail, whereas in the eye lens, skin, spleen, and renal medulla, the HspB5 signals prevail. In the heart, lung, liver, renal cortex, and renal glomeruli, both signals exhibit a similar intensity. A semi-quantitative evaluation of the relative band densities confirms this notion of different relative HspB5L-P44/HspB5 ratios in the studied tissues, varying between < 0.05 and > 10. The numeric values for each studied tissue are given in Fig. 2.

As anticipated from literature data (Tanguay et al. 1993; Klemenz et al. 1993), the 8A7 antibody labeled also HspB1 in a number of these tissues (Fig. 2), that is, however, of little relevance to this report.

HspB5L-P44 in human brains

In order to verify the existence of HspB5L-P44 in human tissues, we analyzed CNS tissues taken at autopsy from three patients with infantile AXD with defined missense mutations in the *GFAP* gene (cf. Methods section). For control purposes, CNS tissues were taken from one patient each with no neuropathology (C1) and with X-linked ALD (C2). Human brain is known to contain HspB5 (Iwaki et al. 1992; Renkawek et al. 1992), the amount of which can be greatly increased in a number of neurological disorders (Iwaki et al. 1992; Renkawek et al. 1992; Lowe et al. 1992a, b), including AXD which is characterized by the deposition of HspB5-containing Rosenthal fibers in astrocytes (Iwaki et al. 1989; Head et al. 1993). All three AXD patients included in this study showed the typical loss of myelin in white matter with many astrocytes with Rosenthal fibers, as opposed to the control patients which had no Rosenthal fibers although the loss of myelin occurred also in the patient with ALD (not shown). Consistent with these histological findings, the three AXD patients exhibited elevated levels of HspB5, preferentially in the white matter as visualized by SDS-PAGE/western blotting using the HspB5-specific antibody, compared to the control patients (Fig. 3, lower panel).

The 8A7 antibody detected HspB5L-P44 in all AXD samples and in the control sample (C1) without neuropathology (Fig. 3, upper panel). In particular, the sample taken from the gray matter of an AXD patient is distinguished by an elevated amount of HspB5L-P44, whereas the samples derived from white matter, or white matter and cortex combined, contained moderate amounts of this protein comparable to that of the control brain without neuropathology (C1). In contrast, the white matter of the control patient with ALD (C2) did not contain detectable amounts of HspB5L-P44. Of note, all brain samples contained HspB1 as detected by the 8A7 antibody.

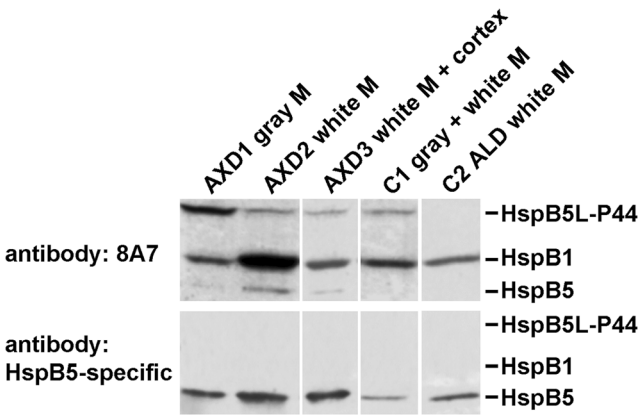

Fig. 3 Occurrence of HspB5L-P44 in human brains. Brain tissues were collected from three patients with AXD with defined missense mutations in the *GFAP* gene (AXD1, AXD3: R416W; AXD2: R239C), and from one individual each without neuropathology (C1) and with ALD (C2) for control purposes. The western blots were stained with the 8A7 antibody or the HspB5-specific antibody, as indicated. M, matter

In summary, HspB5L-P44 can be found also in human tissues as exemplified for the brain. This tentatively suggests that the presence of this protein may be a general feature of many mammalian tissues, although the experimental proof still needs to be provided. Confirming the findings of Fig. 2, the relative amounts of HspB5L-P44 and HspB5 do not seem to correlate.

Regulation of the formation of HspB5L-P44 in response to oxidative stress in endothelial cells

Using the 8A7 antibody, we detected HspB5L-P44 in cultured rat pulmonary arterial endothelial cells which contain also HspB5. Considering the fact that HspB1 formed covalently bonded dimers in oxidative conditions (Zavialov et al. 1998a), we exposed the endothelial cells for 30 min to UV light and determined the formation of the HspB5L-P44 in the following recovery period of up to 24 h (Fig. 4). The formation of HspB5L-P44 was induced in the time period between 1 and 6 h following the exposure to UV light, before returning to normal. In contrast, no major change was seen in the HspB5 band, confirming the above observation according to which the amounts of HspB5L-P44 and HspB5 do not correlate.

We conclude that the formation of HspB5L-P44 is physiologically regulated in live cells. Similarly to HspB1, HspB5 can dimerize in oxidative conditions resulting in the formation of HspB5L-P44.

The exposed position of the 8A7 epitope in spatial models of the α-crystallin domain in HspB5 monomers and dimers

When the signal intensities for HspB5L-P44 obtained with both antibodies are compared to the signals obtained for HspB5, it is evident that the 8A7 antibody exhibits a much stronger affinity towards HspB5L-P44 than the HspB5-specific antibody (cf. Figs. 1, 3). In order to elucidate this antibody behavior, we have mapped the position of the ho-ADP (i) onto a model of the secondary and tertiary structures

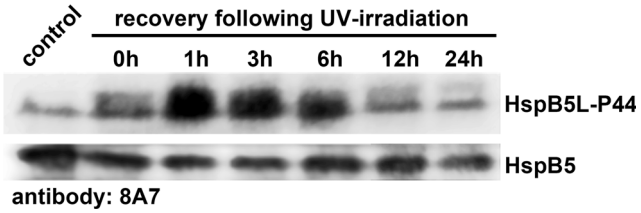

Fig. 4 Physiological regulation of the HspB5L-P44 in response to UV-irradiation in rat pulmonary arterial endothelial cells. Cells grown in 6-well plates were exposed for 30 min to ~240 μW/cm^2 UV light in a biological safety cabinet, and were subsequently allowed to recover in an incubator. At the times indicated, the cells were harvested and processed for SDS-PAGE followed by western blotting, using the 8A7 antibody which stained both HspB5L-P44 and HspB5

of the α-crystallin domain of HspB5 and (ii) onto a model of α-crystallin domain dimers of this protein.

Figure 5(a) shows the aligned sequences of rat and human HspB5 containing the ho-ADP sequences for the 8A7 antibody (green), to which the human HspB1-derived 8A7-ADP is also aligned. Being positioned in the most conserved parts of sHSPs (Fontaine et al. 2003; Benndorf et al. 2014), the ho-ADP (HspB5) and 8A7-ADP (HspB1) sequences differ in just two amino acid residues. This explains both the cross-reactivity of the 8A7 antibody with HspB5 (cf. Figs. 1–4) and the reduced affinity towards HspB5 monomers, compared to the HspB5-specific antibody (cf. Fig. 3).

The prevailing secondary structures in the α-crystallin domain of all studied sHSPs are β-strands which typically assemble into two main β-sheets (Mymrikov et al. 2011). Figure 5(a) illustrates the positions of the various β-strands along the α-crystallin domain sequence, as derived from the "worm"-style X-ray structural model of a single α-crystallin domain of human HspB5 that is shown in Fig. 5(b) (X-ray structure, PDB ID 2WJ7; ref. Bagneris et al. 2009). In this model, the ho-ADP extends from the C-terminal end of β-strand 5 through two small β-strands (designated β-strands 5–2 and 6), to reach the N-terminal end of β-strand 7. In this manner, the ho-ADP forms an additional small β-sheet that protrudes into the space outside the core β-sheet structure (in Fig. 5(b), the ho-ADP segment is labeled green with the single amino acid residues being indicated). Although another model differs slightly (Rajagopal et al. 2015), both models clearly demonstrate that the ho-ADP sequence in HspB5 is located in an exposed position: By protruding out of the core β-sheet structure of the α-crystallin domain, the ho-ADP segment becomes an easily accessible target for the 8A7 antibody thus facilitating its binding.

This feature, however, does not explain the high affinity of the 8A7 antibody towards HspB5L-P44 relative to monomeric HspB5. The key for understanding must reside in the quaternary structure of HspB5L-P44. Therefore, we labeled the two ho-ADP segments in a model of HspB5 α-crystallin domain dimers as shown in Fig. 5(c) (solid-state NMR structural model, PDB ID 2KLR; ref. Jehle et al. 2010). This space-filling model confirms that both ho-ADPs (labeled green and yellow) keep largely their exposed position also in this dimeric complex. Both ho-ADP segments are in an adjacent position with a distance spanning approximately 1 to 5 nm, which is, however, on the short side of the optimal range for antibody binding through both antigen binding sites that typically occurs at an epitope distance of 6–12 nm (Preiner et al. 2014).

Bivalent antibody binding (which is required for high avidity) is a highly complex process, influenced by a number of factors including the flexibility of the antibodies, steric restraints of both antibody and antigen, and other experimental specifics like the polymeric nature and the immobilization of the antigen, with the latter resulting in a high epitope density

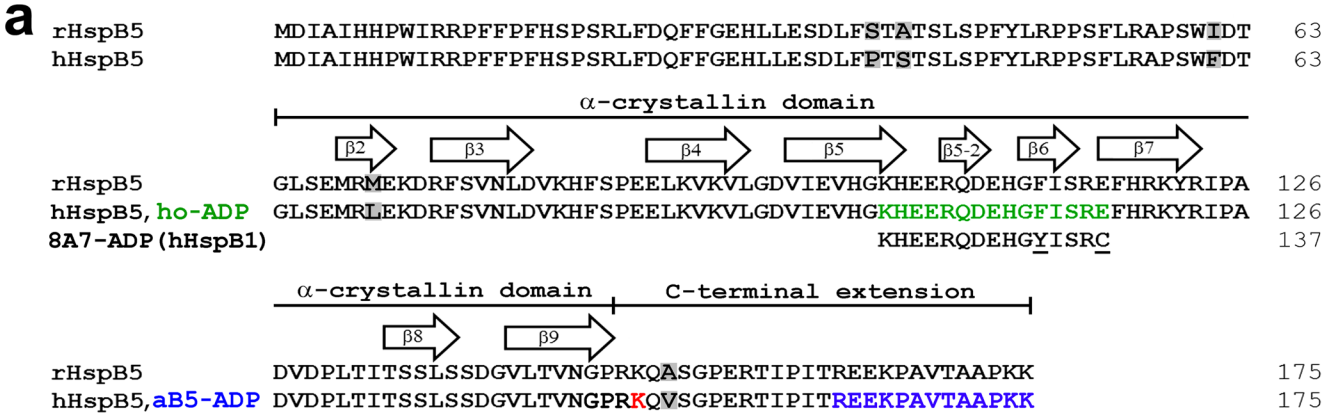
a
rHspB5 MDIAIHHPWIRRPFFPFHSPSRLFDQFFGEHLLESDLFSTATSLSPFYLRPPSFLRAPSWIDT 63
hHspB5 MDIAIHHPWIRRPFFPFHSPSRLFDQFFGEHLLESDLFPTSTSLSPFYLRPPSFLRAPSWFDT 63
α-crystallin domain
β2 β3 β4 β5 β5-2 β6 β7
rHspB5 GLSEMRMEKDRFSVNLDVKHFSPEELKVKVLGDVIEVHGKHEERQDEHGFISREFHRKYRIPA 126
hHspB5, ho-ADP GLSEMRLEKDRFSVNLDVKHFSPEELKVKVLGDVIEVHGKHEERQDEHGFISREFHRKYRIPA 126
8A7-ADP(hHspB1) KHEERQDEHGYISRC 137
α-crystallin domain C-terminal extension
β8 β9
rHspB5 DVDPLTITSSLSSDGVLTVNGPRKQASGPERTIPITREEKPAVTAAPKK 175
hHspB5, aB5-ADP DVDPLTITSSLSSDGVLTVNGPRKQVSGPERTIPITREEKPAVTAAPKK 175

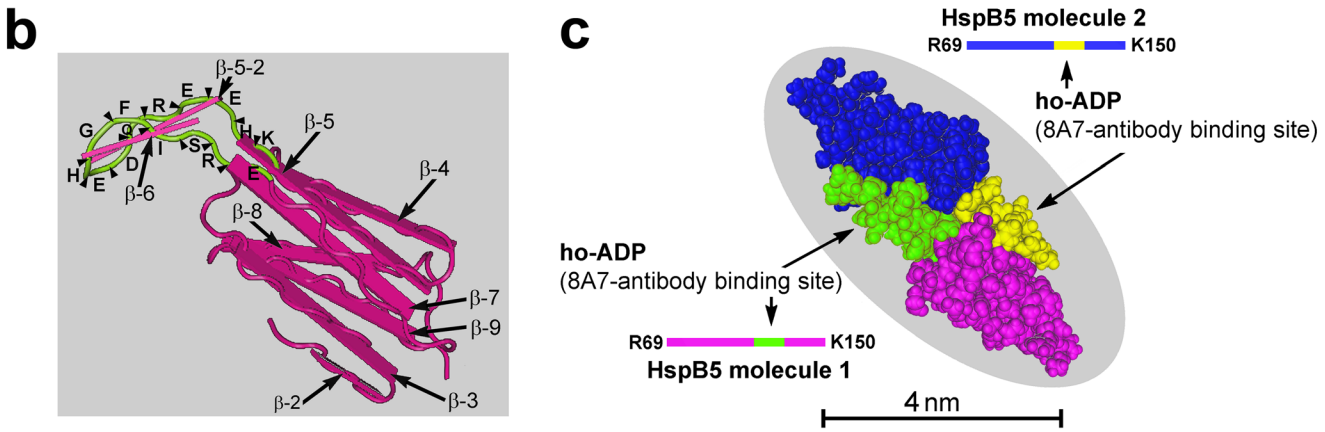
b
β-5-2
β-5
β-4
β-6
β-8
β-7
β-9
β-2
β-3
c
HspB5 molecule 2
R69 K150
ho-ADP
(8A7-antibody binding site)
ho-ADP
(8A7-antibody binding site)
R69 K150
HspB5 molecule 1
4 nm

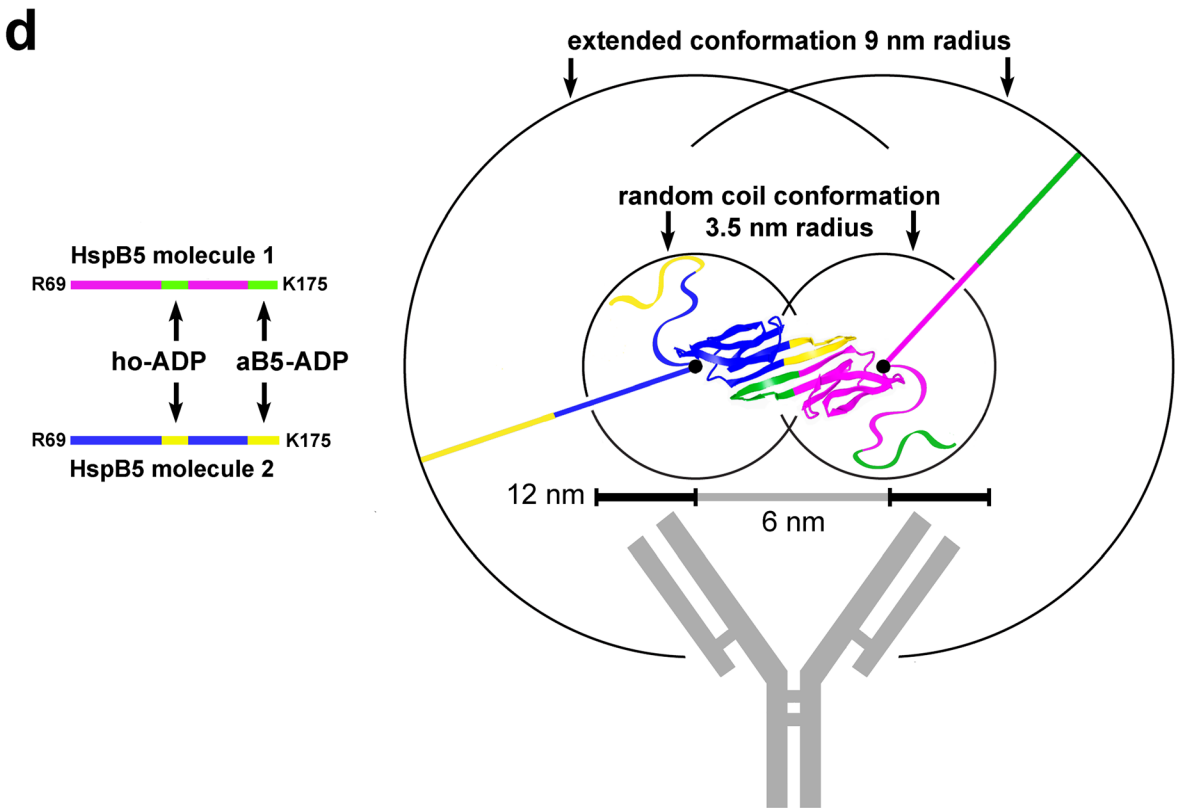
d
HspB5 molecule 1
R69 K175
ho-ADP aB5-ADP
R69 K175
HspB5 molecule 2
extended conformation 9 nm radius
random coil conformation
3.5 nm radius
12 nm
6 nm

◀ **Fig. 5** Antigen determinant peptide (ADP) sequences for two HspB5-recognizing antibodies and their positions in the primary, secondary, tertiary, and quaternary structures of human monomeric and dimeric HspB5. (a) Aligned sequences of rat (rHspB5) and human HspB5 (hHspB5) which differ in five positions (highlighted gray). The ADP for the 8A7 antibody (8A7-ADP, derived from human HspB1) is placed below the homologous site of HspB5 (ho-ADP; labeled green in hHspB5). Both the 8A7-ADP and ho-ADP differ in two positions (underlined in the 8A7-ADP sequence). The ADP of the HspB5-specific antibody (aB5-ADP) is composed of the 13 uttermost C-terminal residues of human HspB5 (labeled blue). The positions of the α-crystallin domain and of the C-terminal extension are indicated as defined previously (Fontaine et al. 2003). The β-strands 2 through 9 are delineated according to the spatial model of the α-crystallin domain of HspB5 as shown in panel b. Lys150, the hindmost C-terminal amino acid residue which is covered by the model shown in panel c, is labeled red. (b) X-ray structure (PDB ID 2WJ7) of the α-crystallin domain of human HspB5 with β-strands 2 to 9 shown as planks. This view features the ho-ADP sequence (green ribbon with the positons of the amino acid residues indicated) which forms a short yet separate β-sheet protruding away from the core β-sheet structure. (c) Space-fill representation of the human HspB5 α-crystallin domain dimer NMR structure (PDB ID 2KLR). The monomers are colored magenta and blue with the corresponding ho-ADP segments green and yellow, respectively. (d) Different quality of the binding sites for both antibodies (ho-ADP vs. aB5-ADP) in the human HspB5 dimer (based on model PDB ID 2KLR). The ho-ADP sites reside in the highly ordered α-crystallin domain, whereas the aB5-ADP sites reside in the extreme end of the disordered and flexible C-terminal extensions which theoretically can move freely in three dimensions within the spherical space delineated by the circles (either in extended or in random coil conformations as indicated), with Lys150 serving as "anchor points" (black dots). HspB5 molecule 1 is colored magenta with both antibody binding sites in green, and HspB5 molecule 2 is colored blue with both antibody binding sites in yellow. To illustrate the size proportion, a stylized antibody is also shown to scale. The measure indicates the range of epitope distances that typically are optimal for bivalent antibody binding (6–12 nm), although with exceptions. In panels c and d, the extreme N- and C-terminal amino acid residues that are included in these models are indicated

(Kaufman and Jain 1992). And even a short distance between the epitopes may enhance bivalent antibody binding, unless steric constraints prevent it (Plückthun and Pack 1997). Some of these factors may enhance the bivalent antibody binding by several orders of magnitude (Crothers and Metzger 1972; Plückthun and Pack 1997) as demonstrated impressively for the bivalent IgG antibody binding on the surface of a Dengue virus resulting in a 20,000-fold increase over monovalent Fab fragments of the same antibody (Edeling et al. 2014).

Another factor contributing to antibody binding is the ability of proteins to refold following the immobilization on blotting membranes. Denatured proteins indeed can refold to a large extent when returned into "physiological" conditions, and several blotting techniques even rely on the correct refolding of the transferred proteins on blotting membranes (Hall 2004; Franke et al. 2009). For urea- and thermally denatured bovine HspB5, it was shown that the secondary, tertiary, and also quaternary structures were largely restored by refolding (Maiti et al. 1988; Raman et al. 1995; Saha and Das 2007), suggesting that also HspB5L-P44 could be partially refolded on the blots shown in Figs. 1–4.

In summary, the experimentally observed high avidity of the 8A7 antibody towards HspB5L-P44 can be explained by a number of factors that include (i) the exposed position of the epitope (ho-ADP) as part of the highly ordered β-sheet structure in the α-crystallin domain of HspB5, (ii) the exposed and adjacent position of both epitopes in HspB5 dimers, (iii) experimental specifics such as the immobilization of the antigen, and (iv) the ability of HspB5 and of its derivative protein species to largely refold on the blotting membrane. Together, these factors make a bivalent binding of HspB5L-P44 by the 8A7 antibody plausible, resulting in the observed high avidity.

Qualitative differences between the epitopes for the 8A7 and the HspB5-specific antibodies in the spatial structure of HspB5 dimers

The above considerations, however, do not explain the relatively poor reactivity of the HspB5-specific antibody towards HspB5L-P44. As noted, the weak signal obtained with the HspB5-specific antibody for HspB5L-P44 contrasts with the strong signal obtained with the 8A7 antibody, if set in relation to the signals obtained for monomeric HspB5. This unexpected antibody behavior may also be explained by the structural model of HspB5 α-crystallin domain dimers, taking into account the nature of the C-terminal extensions which carry the epitope for the HspB5-specific antibody, herein termed the anti-HspB5 antigen determinant peptide (aB5-ADP). This antibody was raised against the 13 uttermost C-terminal amino acid residues of human HspB5, constituting approximately half of the C-terminal extension (labeled blue in Fig. 5(a)) (Bhat et al. 1991). These C-terminal extensions are distinguished by their intrinsically disordered and highly flexible nature which has been studied extensively (Carver et al. 1995; Treweek et al. 2010; Sudnitsyna et al. 2012). This structural characteristic may have negative implications for antibody binding, be it by the intrinsic properties of the C-terminal extensions or by their unpropitious positioning in space.

With regard to the spatial constellation, the C-terminal extensions theoretically can take up any position which is within reach of their length. In an unfolded conformation and with an average length of 0.38 nm for each amino acid residue (Rico et al. 2013) downstream of Lys150 which is the most C-terminal amino acid residue that is covered by the model shown in Fig. 5(c), all 25 downstream amino acid residues would add up to approximately 9 nm length. This length delineates the maximal radii of the two overlapping spheres, and therein the two aB5-ADP segments theoretically can adopt any position using the two Lys150 residues as "anchor points" (Fig. 5(d); Lys150 residues indicated by black dots). According to this model, the distances between both aB5-ADP segments can be estimated to be in the range between

0 nm and maximal 25 nm. Both extreme positions, as well as most intermediate positions, would be outside the optimal range for bivalent antibody binding (6–12 nm), contributing to the poor binding of the HspB5-specific antibody towards HspB5L-P44. Even at a permissive distance, a major fraction of these flexible C-terminal extensions can be expected to adopt conformations and/or relative constellations that are unfavorable for antibody binding.

However, in solution, a random coil conformation of the C-terminal extensions is more probable (Fisher et al. 1999), even though on the blotting membranes the fate of the C-terminal extensions is less certain. In such a random coil conformation, unfolded proteins are best described as Kuhn-type polymers following a random flight model, in which each subsequent amino acid residue is restrained by permissible bond angles only, and the ensemble is statistically distributed (Kuhn 1934; Tanford et al. 1966). According to this model, the 25 C-terminal residues are expected to be broadly distributed between 0 and 6 nm with a statistical average of approximately 3.5 nm (Goldenberg 2003). In Fig. 5(d), this constellation is also visualized by the inner spheres which delineate the average space occupied by the C-terminal extensions in a random coil conformation. Also in this model, a fraction of the possible positions of the aB5-ADP segments would be outside the optimal range for bivalent antibody binding and/or adopt unfavorable spatial conformations and relative constellations, thus attenuating the binding of the HspB5-specific antibody towards HspB5L-P44.

To visualize the size proportions of HspB5L-P44 dimers and of antibodies, a stylized IgG antibody is also shown in Fig. 5(d).

Taken together, on the blotting membrane, these disordered and flexible C-terminal extensions can be expected to adopt an extended or random coil conformation. In any case, the result for antibody binding towards HspB5L-P44 is similar: The bivalent binding by the HspB5-specific antibody will be attenuated (i) by largely unfavorable epitope-epitope distances in the dimeric structure, and/or (ii) by unfavorable conformations and relative constellations of these extensions. Thus, these structural features of the C-terminal extensions provide a rationale for the observed low affinity of the HspB5-specific antibody (and of similar antibodies) towards HspB5L-P44. This antibody property may also provide an explanation for the fact that the HspB5L-P44 was not noticed in previous studies.

Although Fig. 5(c, d) shows the quaternary structure of an HspB5 α-crystallin domain dimer, this model, however, does not feature the covalent bond between the HspB5 monomers, the existence of which can be postulated on the basis of the electrophoretic behavior as shown in Figs. 1–4, and which has not been reported before in naturally occurring HspB5 species. Both the exact position and the chemical nature of this postulated covalent bond remain to be determined.

HspB5 speciation as found in proteome databases

The existence of HspB5L-P44 in rat and human tissues, as described in this study, suggests that HspB5 is subjected to protein speciation, similar to HspB1 (Scheler et al. 1997; Benndorf and Jungblut 2015) or other studied proteins (Jungblut et al. 2016). In order to find further evidence for the speciation of HspB5 in vertebrates, we searched proteomics databases for HspB5 and its derivatives and re-evaluated various two-dimensional gels from earlier published studies.

Among the different proteomics approaches (Schlüter et al. 2009), the two-dimensional gel electrophoresis mass spectrometry (2-DE-MS) top-down method is best suited for the identification of putative HspB5 dimers. In particular, this approach has been used to build a number of well-documented 2D-PAGE databases. Table 1 lists such databases and studies that are based on a total of 11 two-dimensional gel electrophoretic protein patterns from four species (human, rat, mouse, Asiatic toad) and six organs or tissues, with samples containing between one and four spots of HspB5. Comparison of the determined M*r* and pI values reveals the existence of at least ten different HspB5 species in these tissues, in spite of the limited comparability of these data between the databases. Since these studies were not designed to identify the complete set of HspB5 species, the true numbers of HspB5 species in these samples can be expected to be even higher. Identified HspB5 spots with a M*r* smaller than 20 kDa can be assumed to contain truncated proteins. Peptide mass fingerprints of such lower mass HspB5 spots in the mouse eye lens suggest truncation from both the N- and C-terminal ends of the protein (Hoehenwarter et al. 2008). In one study of the human heart, an HspB5 form with an estimated M*r* of 30 kDa was identified that is clearly above the size of the HspB5 monomer (Polden et al. 2011). However, identity of this or any other HspB5 species listed in Table 1 with HspB5L-P44 can be excluded, based on the different masses and isoelectric points.

In summary, in vertebrate tissues, a number of non-canonical HspB5 species exist that have been largely neglected in earlier studies. HspB5 shares this speciation with HspB1 and other studied proteins, thus further supporting the concept of the protein code. HspB5L-P44 as reported in this study is just one non-canonical HspB5 species among others.

Discussion

In recent decades, a number of different modifications of HspB5 have been reported, among them phosphorylation at three sites (Ito et al. 1997, 2001; den Engelsman et al. 2005). Other modifications and variations include O-GlcN-acylation (Roquemore et al. 1996), alternative transcription initiation sites (Macip et al. 1997), addition of a C3-body to the C-terminal lysine (Lin et al. 1997), cross-linking by tissue

Table 1 HspB5 species in 2D-PAGE databases of vertebrate species

Organism	Tissue	No. of spots	Mr (kDa)	pI	Database	Reference
Human	Heart	3	17.6; 30.3; 9.3	7.0; 6.9; 8.4	UCD 2D-PAGE	Polden et al. 2011
Human	Heart	3	23.0; 23.0; 21.5	6.50; 6.51; 6.50	UCD 2D-PAGE	Westbrook et al. 2006
Human	Colorectal epithelial cells	1	16.9	8.5	Swiss 2D-PAGE	Reymond et al. 1997
Human	Testis	1	20.2	6.9	REPRODUCTIVE 2D-PAGE	Guo et al. 2010
Human	Kidney	1	15.6	7.2	Swiss 2D-PAGE	Sarto et al. 1997
Mouse	Lens	1	24	7	–	Jungblut et al. 1998
Mouse	Lens	4	24; 18; 16; 14	7.1; 6.8; 7.2; 7.5	2D-PAGE MPIIB	Hoehenwarter et al. 2008
Mouse	Gastrocnemius muscle	2	21.2; 20.8	6.7; 6.8	Swiss 2D-PAGE	Sanchez et al. 2001
Mouse	Heart	1	20.1	6.8	2D-PAGE MPIIB	Schwab et al. 2011
Rat	Heart	1	21	7.8	FU database	Li et al. 1999
Asiatic toad[a]	Lens	4	14.3; 17.5; 17.4; 18.5	5.5; 6.3; 6.5; 6.5	UCD 2D-PAGE	Keenan et al. 2009

[a] *Bufo gargarizans*

transglutaminase (Merck et al. 1993), carbamylation and acetylation (Lapko et al. 2001), C-terminal truncation (Kamei et al. 2000), glycation (Ortwerth et al. 1992), ubiquitinylation (Goldman and Corbin 1991), and others (reviewed in Groenen et al. 1994; Hanson et al. 2000). The existence of HspB5L-P44, being most likely a naturally occurring covalently bonded HspB5 dimer, further adds to the complex modification pattern of this sHSP, the more so as HspB5L-P44 exists in at least four protein species.

Although HspB5 dimers per se have been known for a long time, notably as building blocks of larger oligomers, all naturally occurring dimers reported to date were formed by association and thus could be dissociated in suitable conditions. A separate finding is the formation of covalently bonded dimers of HspB5 in vitro, together with the closely related HspB4 (αA-crystallin), upon chemical oxidation of the purified proteins (Balasubramanian and Kanwar 2002; Shum et al. 2005). However, mixed dimers of this type, which formed only in harsh oxidative conditions, do not seem to exist in a physiological environment in tissues, the more so as the expression of the HspB4 gene (*CRYAA*) is restricted to the eye lens. Nevertheless, the existence of these dimers demonstrates the possibility of HspB5 forming covalently bonded dimers. The putative covalently bonded HspB5 dimers reported here are distinguished by the fact that they occur naturally in a number of mammalian tissues.

The related HspB1 is also subject to numerous modifications that may explain the highly complex HspB1 species patterns (with ~60 HspB1 species) found in a few studied experimental systems using suitable analytical tools (Benndorf and Jungblut 2015). Known modifications of HspB1 include the formation of covalently bonded HspB1 dimers via a sulfur bridge in oxidative conditions (Zavialov et al. 1998a, b). HspB5, in contrast, has no cysteine in its primary sequence (cf. Fig 5(a)) thus excluding the involvement of a sulfur bridge in the formation of HspB5L-P44. Instead, HspB5L-P44 must be formed by another bond. A candidate is the dityrosine bond which has been identified in the mixed HspB4/HspB5 dimers that formed upon chemical oxidation in vitro (Balasubramanian and Kanwar 2002; Shum et al. 2005). Also, HspB8 forms covalently bonded dimers, albeit the nature of this bond is not known (Benndorf et al. 2001). In summary, the property "covalently bonded dimer formation" is shared by some sHSPs including HspB5, HspB1, and HspB8, irrespective of the differing nature of the involved chemical bonds.

The fact that a number of mutations in the *CRYAB* gene in patients are associated with cataracts in the lens of the eye and/or with various myopathies including myofibrillar or desmin-related myopathy, dilated cardiomyopathy and hypertonic infantile muscular dystrophy (Datskevich et al. 2012; Benndorf 2010; Benndorf et al. 2014) raise the question of the involvement of HspB5L-P44 in these disorders. For example, mutant HspB5 may result in abnormal formation of HspB5L-P44, or in formation of HspB5L-P44 with abnormal properties, eventually contributing to the etiology of these disorders.

As demonstrated in this study, HspB5-specific antibodies raised against epitopes in the C-terminal extensions are poorly suitable to detect HspB5L-P44 species on western blots. This implies the possibility that most if not all studies using this or similar antibodies in the past have missed HspB5L-P44, and potentially missed also important aspects of the regulation and biological function of HspB5 and of its derivatives. The fact that the relative amounts of HspB5L-P44 and HspB5 do not

correlate in the various tissues and cells (cf. Figs. 2–4) indeed suggests such a specific regulation of the HspB5-derived species. Unfortunately, no data on possible functional implications are available at this time.

Using published data on the structural features both of the HspB5 α-crystallin domain dimers and of the intrinsically disordered and flexible C-terminal extensions, we provide an explanation for the surprising difference by which the 8A7 antibody and the HspB5-specific antibody label HspB5L-P44, relative to monomeric HspB5. The relative affinities of the antibodies used in this study towards HspB5L-P44 and HspB5 are not known and may differ by orders of magnitude. This implies that at this time no conclusions can be drawn on the amounts of HspB5L-P44 in these tissues, relative to monomeric HspB5.

The formation of HspB5L-P44 with its four species represents another example of protein speciation (Jungblut et al. 2008). An additional reason why these protein species were not identified earlier is the limitation of the bottom-up proteomics. As long as not all spots of a 2-DE pattern are investigated by mass spectrometry, 2-DE-MS has to be complemented by two-dimensional immunoblotting to detect the various species of a protein of interest. Such protein species may be regulated in a protein species-specific manner, e.g., during the development of diseases, and functional consequences can be better deduced as compared to the fuzzy data obtained at the protein level by the bottom-up approaches. Hereby the protein speciation discourse directly leads to the protein code concept (Sims and Reinberg 2008; Benndorf and Jungblut 2015; Jungblut et al. 2016), and HspB5 with all of its derivatives (species), including HspB5L-P44, well suites this picture, even in the absence of known functional consequences.

In conclusion, we provide electrophoretic and immunological evidence for a novel 44-kDa HspB5-related protein we term HspB5L-P44. This protein exists in at least four species and is most likely a covalently bonded HspB5 dimer. With this putative HspB5 dimer occurring in a number of rat tissues and human brains, it can be concluded that it occurs widely in mammalian tissues. The relative amounts of HspB5 and HspB5L-P44 do not correlate in the tested tissues, suggesting a physiological regulation of the formation of HspB5L-P44 independent of HspB5. At present, no data on possible functional implications on HspB5L-P44 are available. The fact that previous studies on HspB5 have missed the HspB5L-P44 species is attributable to (i) the unique properties of the HspB1-/HspB5-specific 8A7 antibody that was used in the present study, but was rarely used in earlier studies, and to (ii) the limitations of bottom-up proteomics. With these newly HspB5-derived species, HspB5 represents another example supporting the concept of the protein code, according to which the expression of genes is reflected only by the complete set of the derived protein species.

Compliance with ethical standards

Rats were housed in animal facilities accredited by the American Association of Laboratory Animal Care, with free access to pelleted food and water. Housing and all procedures were conducted in accordance with the guidelines of the National Institute of Health and were approved by the University of Michigan Committee on Use and Care of Animals (approval nos. 7835 and 7989). Rats were euthanized by inhalation of carbon dioxide in accordance with the American Veterinary Medical Association guidelines on euthanasia.

References

Aquilina JA, Shrestha S, Morris AM, Ecroyd H (2013) Structural and functional aspects of hetero-oligomers formed by the small heat shock proteins αB-crystallin and HSP27. J Biol Chem 288:13602–13609

Bagnéris C, Bateman OA, Naylor CE, Cronin N, Boelens WC, Keep NH, Slingsby C (2009) Crystal structures of alpha-crystallin domain dimers of alphaB-crystallin and Hsp20. J Mol Biol 392:1242–1252 Erratum in: J Mol Biol (2009) 394:588

Balasubramanian D, Kanwar R (2002) Molecular pathology of dityrosine cross-links in proteins: structural and functional analysis of four proteins. Mol Cell Biochem 234-235:27–38

Behlke J, Dube P, van Heel M, Wieske M, Hayess K, Benndorf R, Lutsch G (1995) Supramolecular structure of the small heat shock protein Hsp25. Progr Colloid Polym Sci 99:87–93

Benndorf R (2010) HSPB1 and HSPB8 mutations in neuropathies. In: Simon S, Arrigo A-P (eds) Small stress proteins and human diseases. Nova Science Publishers, New York, pp 301–324

Benndorf R, Engel K, Gaestel M (2000) Analysis of small Hsp phosphorylation. Methods Mol Biol 99:431–445

Benndorf R, Hayess K, Stahl J, Bielka H (1992) Cell-free phosphorylation of the murine small heat-shock protein hsp25 by an endogenous kinase from Ehrlich ascites tumor cells. Biochim Biophys Acta 1136:203–207

Benndorf R, Jungblut PR (2015) Reconsidering old data: non-canonical HspB1 species and the enigma of the cytoskeletal function of HspB1. In: Tanguay RM, Hightower LE (eds) The big book on small heat shock proteins. Springer Verlag, Heidelberg, pp 471–486

Benndorf R, Martin JL, Kosakovsky Pond SL, Wertheim JO (2014) Neuropathy- and myopathy-associated mutations in human small heat shock proteins: characteristics and evolutionary history of the mutation sites. Mutat Res Rev Mutat Res 761:15–30

Benndorf R, Sun X, Gilmont RR, Biederman KJ, Molloy MP, Goodmurphy CW, Cheng H, Andrews PC, Welsh MJ (2001) HSP22, a new member of the small heat shock protein superfamily, interacts with mimic of phosphorylated HSP27 (^{3D}HSP27). J Biol Chem 276:26753–26761

Bhat SP, Horwitz J, Srinivasan A, Ding L (1991) Alpha B-crystallin exists as an independent protein in the heart and in the lens. Eur J Biochem 202:775–781

Bitar KN, Kaminski MS, Hailat N, Cease KB, Strahler JR (1991) Hsp27 is a mediator of sustained smooth muscle contraction in response to bombesin. Biochem Biophys Res Commun 181:1192–1200

Carver JA, Esposito G, Schwedersky G, Gaestel M (1995) 1H NMR spectroscopy reveals that mouse Hsp25 has a flexible C-terminal extension of 18 amino acids. FEBS Lett 369:305–310

Crothers DM, Metzger H (1972) The influence of polyvalency on the binding properties of antibodies. Immunochemistry 9:341–357

Datskevich PN, Nefedova VV, Sudnitsyna MV, Gusev NB (2012) Mutations of small heat shock proteins and human congenital diseases. Biochemistry (Mosc) 77:1500–1514

Delbecq SP, Rosenbaum JC, Klevit RE (2015) A mechanism of subunit recruitment in human small heat shock protein oligomers. Biochemistry 54:4276–4284

den Engelsman J, Gerrits D, de Jong WW, Robbins J, Kato K, Boelens WC (2005) Nuclear import of alphaB-crystallin is phosphorylation-dependent and hampered by hyperphosphorylation of the myopathy-related mutant R120G. J Biol Chem 280:37139–37148

Dubin RA, Wawrousek EF, Piatigorsky J (1989) Expression of the murine alpha B-crystallin gene is not restricted to the lens. Mol Cell Biol 9:1083–1091

Edeling MA, Austin SK, Shrestha B, Dowd KA, Mukherjee S, Nelson CA, Johnson S, Mabila MN, Christian EA, Rucker J, Pierson TC, Diamond MS, Fremont DH (2014) Potent dengue virus neutralization by a therapeutic antibody with low monovalent affinity requires bivalent engagement. PLoS Pathog 10:e1004072

Elliott JL, Der Perng M, Prescott AR, Jansen KA, Koenderink GH, Quinlan RA (2013) The specificity of the interaction between αB-crystallin and desmin filaments and its impact on filament aggregation and cell viability. Philos Trans R Soc Lond Ser B Biol Sci 368: 20120375

Fisher TE, Oberhauser AF, Carrion-Vazquez M, Marszalek PE, Fernandez JM (1999) The study of protein mechanics with the atomic force microscope. Trends Biochem Sci 24:379–384

Fontaine JM, Rest JS, Welsh MJ, Benndorf R (2003) The sperm outer dense fiber protein is the 10th member of the superfamily of mammalian small stress proteins. Cell Stress Chaperones 8:62–69

Franke C, Gräfe D, Bartsch H, Bachmann M (2009) Use of non-radioactive detection method for north- and southwestern blot. In: Methods in molecular biology (Clifton, N.J.), vol 536, pp 441–449

Gilmont RR, Dardano A, Engle JS, Adamson BS, Welsh MJ, Li T, Remick DG, Smith DJ Jr, Rees RS (1996) TNF-alpha potentiates oxidant and reperfusion-induced endothelial cell injury. J Surg Res 61:175–182

Goldenberg DP (2003) Computational simulation of the statistical properties of unfolded proteins. J Mol Biol 326:1615–1633

Goldman JE, Corbin E (1991) Rosenthal fibers contain ubiquitinated alpha B-crystallin. Am J Pathol 139:933–938

Groenen PJ, Merck KB, de Jong WW, Bloemendal H (1994) Structure and modifications of the junior chaperone alpha-crystallin. From lens transparency to molecular pathology. Eur J Biochem 225:1–19

Guess A, Agrawal S, Wei CC, Ransom RF, Benndorf R, Smoyer WE (2010) Dose- and time-dependent glucocorticoid receptor signaling in podocytes. Am J Physiol Renal Physiol 299:F845–F853

Guess AJ, Ayoob R, Chanley M, Manley J, Cajaiba MM, Agrawal S, Pengal R, Pyle AL, Becknell B, Kopp JB, Ronkina N, Gaestel M, Benndorf R, Smoyer WE (2013) Crucial roles of the protein kinases MK2 and MK3 in a mouse model of glomerulonephritis. PLoS One 8(1):e54239

Guo X, Zhao C, Wang F, Zhu Y, Cui Y, Zhou Z, Huo R, Sha J (2010) Investigation of human testis protein heterogeneity using 2-dimensional electrophoresis. J Androl 31:419–429

Hall RA (2004) Studying protein-protein interactions via blot overlay or far western blot. Methods Mol Biol 261:167–174

Hanson SR, Hasan A, Smith DL, Smith JB (2000) The major in vivo modifications of the human water-insoluble lens crystallins are disulfide bonds, deamidation, methionine oxidation and backbone cleavage. Exp Eye Res 71:195–207

Haslbeck M, Peschek J, Buchner J, Weinkauf S (2016) Structure and function of α-crystallins: traversing from in vitro to in vivo. Biochim Biophys Acta 1860:149–166

Head MW, Corbin E, Goldman JE (1993) Overexpression and abnormal modification of the stress proteins alpha B-crystallin and HSP27 in Alexander disease. Am J Pathol 143:1743–1753

Hirano S, Rees RS, Yancy SL, Welsh MJ, Remick DG, Yamada T, Hata J, Gilmont RR (2004) Endothelial barrier dysfunction caused by LPS correlates with phosphorylation of HSP27 in vivo. Cell Biol Toxicol 20:1–14

Hoehenwarter W, Tang Y, Ackermann R, Pleissner KP, Schmid M, Stein R, Zimny-Arndt U, Kumar NM, Jungblut PR (2008) Identification of proteins that modify cataract of mouse eye lens. Proteomics 8: 5011–5024

Ito H, Kamei K, Iwamoto I, Inaguma Y, Nohara D, Kato K (2001) Phosphorylation-induced change of the oligomerization state of alpha B-crystallin. J Biol Chem 276:5346–5352

Ito H, Okamoto K, Nakayama H, Isobe T, Kato K (1997) Phosphorylation of alphaB-crystallin in response to various types of stress. J Biol Chem 272:29934–29941

Iwaki T, Iwaki A, Tateishi J, Sakaki Y, Goldman JE (1993) Alpha B-crystallin and 27-kd heat shock protein are regulated by stress conditions in the central nervous system and accumulate in Rosenthal fibers. Am J Pathol 143:487–495

Iwaki T, Kume-Iwaki A, Liem RK, Goldman JE (1989) αB-crystallin is expressed in non-lenticular tissues and accumulates in Alexander's disease brain. Cell 57:71–78

Iwaki T, Wisniewski T, Iwaki A, Corbin E, Tomokane N, Tateishi J, Goldman JE (1992) Accumulation of alpha B-crystallin in central nervous system glia and neurons in pathologic conditions. Am J Pathol 140:345–356

Jehle S, Rajagopal P, Bardiaux B, Markovic S, Kuhne R, Stout JR, Higman VA, Klevit RE, Van Rossum BJ, Oschkinat H (2010) Solid-state nmr and saxs studies provide a structural basis for the activation of alphab-crystallin oligomers. Nat Struct Mol Biol 17: 1037–1042

Jia Y, Ransom RF, Shibanuma M, Liu C, Welsh MJ, Smoyer WE (2001) Identification and characterization of hic-5/ARA55 as an hsp27 binding protein. J Biol Chem 276:39911–39918

Jungblut PR, Holzhütter HG, Apweiler R, Schlüter H (2008) The speciation of the proteome. Chem Cent J 2:16

Jungblut PR, Otto A, Favor J, Löwe M, Müller E-C, Kastner M, Sperling K, Klose J (1998) Identification of the mouse crystallins in 2D protein patterns by sequencing and mass spectrometry. Application to cataract mutants. FEBS Lett 435:131–137

Jungblut PR, Thiede B, Schlüter H (2016) Towards deciphering proteomes via the proteoform, protein speciation, moonlighting and protein code concepts. J Proteome 134:1–4

Kamei A, Hamaguchi T, Matsuura N, Iwase H, Masuda K (2000) Post-translational modification of alphaB-crystallin of normal human lens. Biol Pharm Bull 23:226–230

Kampinga HH, Hageman J, Vos MJ, Kubota H, Tanguay RM, Bruford EA, Cheetham ME, Chen B, Hightower LE (2009) Guidelines for the nomenclature of the human heat shock proteins. Cell Stress Chaperones 14:105–111

Kato K, Shinohara H, Kurobe N, Inaguma Y, Shimizu K, Ohshima K (1991) Tissue distribution and developmental profiles of immunoreactive alpha B crystallin in the rat determined with a sensitive immunoassay system. Biochim Biophys Acta 1074:201–208

Kaufman EN, Jain RK (1992) Effect of bivalent interaction upon apparent antibody affinity: experimental confirmation of theory using fluorescence photobleaching and implications for antibody binding assays. Cancer Res 52:4157–4167

Keenan J, Elia G, Dunn MJ, Orr DF, Pierscionek BK (2009) Crystallin distribution patterns in concentric layers from toad eye lens. Proteomics 9:5340–5349

Klemenz R, Andres AC, Fröhli E, Schäfer R, Aoyama A (1993) Expression of the murine small heat shock proteins hsp25 and αB-crystallin in the absence of stress. J Cell Biol 120:639–645

Klemenz R, Fröhli E, Steiger RH, Schäfer R, Aoyama A (1991) Alpha B-crystallin is a small heat shock protein. Proc Natl Acad Sci U S A 88: 3652–3656

Kuhn W (1934) Über die Gestalt fadenförmiger Moleküle in Lösungen. Kolloid Z 68:2–15

Lapko VN, Smith DL, Smith JB (2001) In vivo carbamylation and acetylation of water-soluble human lens alphaB-crystallin lysine 92. Protein Sci 10:1130–1136

Li X-P, Pleißner K-P, Scheler C, Regitz-Zagrosek V, Salnikow J, Jungblut P (1999) A two-dimensional electrophoresis database of rat heart proteins. Electrophoresis 20:891–897

Lin P, Smith DL, Smith JB (1997) In vivo modification of the C-terminal lysine of human lens alphaB-crystallin. Exp Eye Res 65:673–680

Lowe J, Errington DR, Lennox G, Pike I, Spendlove I, Landon M, Mayer RJ (1992b) Ballooned neurons in several neurodegenerative diseases and stroke contain alpha B crystallin. Neuropathol Appl Neurobiol 18:341–350

Lowe J, McDermott H, Pike I, Spendlove I, Landon M, Mayer RJ (1992a) Alpha B crystallin expression in non-lenticular tissues and selective presence in ubiquitinated inclusion bodies in human disease. J Pathol 166:61–68

Lutsch G, Vetter R, Offhauss U, Wieske M, Gröne HJ, Klemenz R, Schimke I, Stahl J, Benndorf R (1997) Abundance and location of the small heat shock proteins HSP25 and alphaB-crystallin in rat and human heart. Circulation 96:3466–3476

Macip S, Mezquita C, Mezquita J (1997) Alternative transcriptional initiation and alternative use of polyadenylation signals in the alphaB-crystallin gene expressed in different chicken tissues. Gene 187: 253–257

Maiti M, Kono M, Chakrabarti B (1988) Heat-induced changes in the conformation of alpha- and beta-crystallins: unique thermal stability of alpha-crystallin. FEBS Lett 236:109–114

Merck KB, Groenen PJ, Voorter CE, de Haard-Hoekman WA, Horwitz J, Bloemendal H, de Jong WW (1993) Structural and functional similarities of bovine alpha-crystallin and mouse small heat-shock protein. A family of chaperones. J Biol Chem 268:1046–1052

Mörner CT (1893) Untersuchungen der Proteinsubstanzen in *lichtbrechenden* Medien des Auges. Hoppe-Seylers. Z Physiol Chem 18:61–106

Mymrikov EV, Seit-Nebi AS, Gusev NB (2011) Large potentials of small heat shock proteins. Physiol Rev 91:1123–1159

Ortwerth BJ, Slight SH, Prabhakaram M, Sun Y, Smith JB (1992) Site-specific glycation of lens crystallins by ascorbic acid. Biochim Biophys Acta 1117:207–215

Plückthun A, Pack P (1997) New protein engineering approaches to multivalent and bispecific antibody fragments. Immunotechnology 3: 83–105

Polden J, McManus CA, Dos Remedios C, Dunn MJ (2011) A 2-D gel reference map of the basic human heart proteome. Proteomics 11: 3582–3586

Preiner J, Kodera N, Tang J, Ebner A, Brameshuber M, Blaas D, Gelbmann N, Gruber HJ, Ando T, Hinterdorfer P (2014) IgGs are made for walking on bacterial and viral surfaces. Nat Commun 5: 4394

Rajagopal P, Tse E, Borst AJ, Delbecq SP, Shi L, Southworth DR, Klevit RE (2015) A conserved histidine modulates HSPB5 structure to trigger chaperone activity in response to stress-related acidosis. elife 4. doi: https://doi.org/10.7554/eLife.07304

Raman B, Ramakrishna T, Rao CM (1995) Rapid refolding studies on the chaperone-like alpha-crystallin. Effect of alpha-crystallin on refolding of beta- and gamma-crystallins. J Biol Chem 270: 19888–19892

Rico F, Rigato A, Picas L, Scheuring S (2013) Mechanics of proteins with a focus on atomic force microscopy. J Nanobiotechnol 11(Suppl 1): S3. https://doi.org/10.1186/1477-3155-11-S1-S3

Renkawek K, de Jong WW, Merck KB, Frenken CW, van Workum FP, Bosman GJ (1992) Alpha B-crystallin is present in reactive glia in Creutzfeldt-Jakob disease. Acta Neuropathol (Berl) 83:324–327

Reymond MA, Sanchez J-C, Hughes GJ, Riese J, Tortola S, Peinado MA, Kirchner T, Hohenberger W, Hochstrasser DF, Kockerling F (1997) Standardized characterization of gene expression in human colorectal epithelium by two-dimensional electrophoresis. Electrophoresis 18:2842–2848

Roquemore EP, Chevrier MR, Cotter RJ, Hart GW (1996) Dynamic O-GlcNAcylation of the small heat shock protein alpha B-crystallin. Biochemistry 35:3578–3586

Saha S, Das KP (2007) Unfolding and refolding of bovine alpha-crystallin in urea and its chaperone activity. Protein J 26:315–326

Sanchez JC, Chiappe D, Converset V, Hoogland C, Binz PA, Paesano S, Appel RD, Wang S, Sennitt M, Nolan A, Cawthorne MA, Hochstrasser DF (2001) The mouse SWISS-2DPAGE database: a tool for proteomics study of diabetes and obesity. Proteomics 1:136–163

Sarto C, Marocchi A, Sanchez J-C, Giannone D, Frutiger S, Golaz O, Wilkins MR, Doro G, Cappellano F, Hughes GJ, Hochstrasser DF, Mocarelli P (1997) Renal cell carcinoma and normal kidney protein expression. Electrophoresis 18:599–604

Scheler C, Müller EC, Stahl J, Müller-Werdan U, Salnikow J, Jungblut P (1997) Identification and characterization of heat shock protein 27 protein species in human myocardial two- dimensional electrophoresis patterns. Electrophoresis 18:2823–2831

Schlüter H, Apweiler R, Holzhütter HG, Jungblut PR (2009) Finding one's way in proteomics: a protein species nomenclature. Chem Cent J 9:3–11

Schwab K, Neumann B, Vignon-Zellweger N, Fischer A, Jungblut PR, Stein R, Scheler C, Theuring F (2011) Dietary phytoestrogen supplementation induces sex differences in the myocardial protein pattern of mice: a comparative proteomics study. Proteomics 11:3887–3904

Shum WK, Maleknia SD, Downard KM (2005) Onset of oxidative damage in alpha-crystallin by radical probe mass spectrometry. Anal Biochem 344:247–256

Sims RJIII, Reinberg D (2008) Is there a code embedded in proteins that is based on posttranslational modifications? Nat Rev 9:1–6

Smoyer WE, Ransom R, Harris RC, Welsh MJ, Lutsch G, Benndorf R (2000) Ischemic acute renal failure induces differential expression of small heat shock proteins. J Am Soc Nephrol 11:211–221

Sudnitsyna MV, Mymrikov EV, Seit-Nebi AS, Gusev NB (2012) The role of intrinsically disordered regions in the structure and functioning of small heat shock proteins. Curr Protein Pept Sci 13:76–85

Tanford C, Kawahara K, Lapanje S (1966) Proteins in 6-M guanidine hydrochloride. Demonstration of random coil behavior. J Biol Chem 241:1921–1923

Tanguay RM, Wu Y, Khandjian EW (1993) Tissue-specific expression of heat shock proteins of the mouse in the absence of stress. Dev Genet 14:112–118

Treweek TM, Rekas A, Walker MJ, Carver JA (2010) A quantitative NMR spectroscopic examination of the flexibility of the C-terminal extensions of the molecular chaperones, αA- and αB-crystallin. Exp Eye Res 91:691–699

van de Bovenkamp M, Groothuis GM, Meijer DK, Slooff MJ, Olinga P (2006) Human liver slices as an in vitro model to study toxicity-induced hepatic stellate cell activation in a multicellular milieu. Chem Biol Interact 162:62–69

Westbrook JA, Wheeler JX, Wait R, Welson SY, Dunn MJ (2006) The human heart proteome: two-dimensional maps using narrow-range immobilised pH gradients. Electrophoresis 27:1547–1555

Zavialov A, Benndorf R, Ehrnsperger M, Zav'yalov V, Dudich I, Buchner J, Gaestel M (1998a) The effect of the intersubunit disulfide bond on the structural and functional properties of the small heat shock protein Hsp25. Int J Biol Macromol 22:163–173

Zavialov AV, Gaestel M, Korpela T, Zav'yalov VP (1998b) Thiol/disulfide exchange between small heat shock protein 25 and glutathione. Biochim Biophys Acta 1388:123–132